Theoretical Studies of the Structure and Molecular Dynamics of a Peptide Crystal†

David H. Kitson and Arnold T. Hagler*
The Agouron Institute, 505 Coast Boulevard South, La Jolla, California 92037
Received October 14, 1987; Revised Manuscript Received February 8, 1988

ABSTRACT: Energy minimizations and molecular dynamics simulations have been performed on the cyclic peptide *cyclo*-(Ala-Pro-D-Phe)$_2$ in both the isolated and crystal states. The results of these calculations have been analyzed, both to investigate our ability to reproduce experimental data (structure and vibrational and NMR spectra) and to investigate the effects of environment on the energy, structure, and dynamics of peptides. Comparison of the minimized and time-averaged crystal systems with the experimental peptide structure shows that the calculations have closely reproduced the experimental structure. Molecular dynamics of the isolated molecule has led to a new conformation, which is $\approx$8.5 kcal/mol more stable than the conformation that exists in the crystal, the latter conformation being stabilized by intermolecular (packing) forces. This illustrates the considerable effect that environment can have on the conformation of peptides. The crystal environment has also been shown to significantly reduce the dynamic conformational fluctuations seen for the isolated molecule. The behavior of the peptide during the isolated simulation also supports the experimental NMR observation of a symmetric structure that differs from the asymmetric, instantaneous structures which characterize the molecule during the dynamics. Calculations of vibrational frequencies of the peptide in the crystal and isolated states show the expected shifts in bond-stretching frequencies due to intermolecular interactions. Finally, we have calculated NMR coupling constants from the dynamics simulation of the isolated peptide and have compared these with the experimental values. This has led to a possible reinterpretation of the experimental data.

Computer simulations are playing an increasingly important role in the study of the structural and dynamic properties of biomolecular systems. An assessment of the ability of these simulations to reproduce experimental data is a vital step in the development of these methods. Cyclic peptides provide an excellent source of experimental data for this purpose.

Cyclic peptides have been an intensively studied class of molecules by both experimental methods [including NMR spectroscopy (Deslauriers & Smith, 1980; Kessler, 1982) and diffraction techniques (Karle, 1981)] and theoretical methods. These peptides have been studied for a variety of reasons: There are many biologically important cyclic peptides, such as valinomycin (Duax et al., 1972) (a depsipeptide antibiotic), gramicidin S (Liquori et al., 1966) (an antibiotic), antamanide (Karle et al., 1973) (an antidote to the toxins of the poisonous mushroom *Amanita phalloides*), and vasopressin (du Vigneaud, 1956) (a neurohypophyseal hormone), and their biological properties are critically dependent on their conformation; the cyclic nature limits the conformational freedom of the molecule and makes it more amenable to experimental or theoretical conformational studies; cyclic peptides provide good models for turns in proteins (Rose et al., 1985). We have several objectives in applying computer simulation techniques such as energy minimization or molecular dynamics to the study of the crystal structures of small peptides. The first objective is to use these crystal systems to test the adequacy and validity of current theoretical methodology (Williams, 1965; Momany et al., 1974; Hagler et al., 1979b; Dauber & Hagler, 1980; Hall & Pavitt, 1984; Hagler, 1985) to probe the structural, energetic, and dynamic properties of peptides and proteins. Second, the nature of the crystal structure itself and the effects of the crystal environment on these physical properties of peptides present several interesting questions: How much strain is induced on incorporation of a flexible peptide into a lattice? What are the effects on entropy and dynamic fluctuations? What is the balance of intra- and intermolecular (packing) forces that give rise to the observed crystal structure? How do static or minimized results compare with time-averaged or dynamic properties? Finally, we would like to utilize experimental observables such as vibrational and NMR spectra in the assessment of the validity of the potential energy surface as reflected in the dynamic and minimized structures and corresponding spectral parameters. In addition, the environmental effects on these latter properties of a peptide are equally intriguing and are amenable to both experimental and theoretical investigations.

The achievement of these objectives requires an extensive study of a large variety of peptide systems (Hagler et al., 1979b). As a first step in this task, we present here a study of the cyclic peptide *cyclo*-(Ala-Pro-D-Phe)$_2$. We have calculated the time-averaged structure and energy and structural fluctuations of this molecule in its crystal environment and of the isolated molecule. Thus, we can, for the first time, address in detail the conformational and dynamic effects of lattice interactions and compare to experiment. We have also carried out a lattice energy minimization and minimized the isolated molecule, and we have investigated the environmental effects as well as compared static and dynamic structures. The vibrational spectrum of the isolated molecule has been calculated, and the calculation of the same spectrum in the crystal has allowed us to predict shifts in the vibrational modes due to the balance between intermolecular and intramolecular forces for the first time. Finally, NMR coupling constants have been calculated, from both the time-averaged dynamic structure of the peptide in vacuo and the minimized structure, and these have been compared with the experimental coupling constants, while the time-averaged and minimized structures have been compared with the model proposed for the peptide

† This work was supported by Grant DMB 8510865 from the National Science Foundation and by Grant GM 30793 from the National Institutes of Health. Grants of computer time (on the Cray X-MP/48 at the San Diego Supercomputer Center) were provided by the National Science Foundation (Grant PCM 8421273) and by Cray Research Inc.

0006-2960/88/0427-5246$01.50/0

based on the experimental NMR data (Kopple et al., 1974).

Traditionally, most studies of the conformations of peptides in crystals, and validation of force fields by comparison with crystal structures, have relied on the use of energy minimization (Hagler et al., 1979b; Dauber & Hagler, 1980; Hall & Pavitt, 1984; Hagler, 1985). The molecules in a crystal are not, however, in rigid, static conformations but are constantly fluctuating due to the thermal motion of the atoms, and the X-ray crystal structure of small peptides gives a wealth of highly accurate information, not only on the positions of the atoms but also on these thermal motions in the form of the atomic temperature factors. Because the crystal has this dynamic nature, a comparison of a molecular dynamics trajectory with the full range of data available from the experimental X-ray structure affords us an opportunity to test the techniques and force fields more rigorously and against additional observables than if we rely on minimizations alone. The molecular dynamics method has been used in several studies of the dynamic properties of isolated peptides, including the peptide hormones lysine vasopressin (Hagler et al., 1985), a nonapeptide, and GnRH (Struthers et al., 1985), a decapeptide, and these studies have demonstrated a considerable conformational flexibility for these molecules. Molecular dynamics simulations have also been carried out on isolated proteins (McCammon et al., 1977; Northrup et al., 1980; Levitt, 1983; Ichiye & Karplus, 1983; Åqvist et al., 1985, 1986) and on proteins in their crystal environments (van Gunsteren et al., 1983; Haneef et al., 1985; Berendsen et al., 1987; Avbelj et al., unpublished experiments). For these simulations of isolated molecules there is not, however, any source of accurate experimental data on the dynamic properties of the system, and in the case of protein crystals the dynamic data are of considerably less accuracy than the structural data (van Gunsteren et al., 1983; Kuriyan et al., 1986). As we stated above, accurate dynamic data are available from the X-ray studies of crystals of small peptides, and we can now perform a more rigorous evaluation of the accuracy of our force field and investigate the nature of the crystal structure and the effects of the crystal environment on peptide conformation and dynamics by carrying out simulations of these crystals. To our knowledge, this is the first such calculation on a system of this size and for which experimental data are available of accuracy comparable to that available for small molecules. Given that we have an accurate force field, we can then begin to answer questions related to the effects of thermal motion by a comparison of minimum energy structures and time-averaged dynamics structures. We can also use dynamics to look at the properties of the isolated molecule and can investigate the nature of the crystal forces by a comparison of the crystal and the isolated molecule. We cannot, of course, rely on the results of a simulation of only one crystal, and a complete validation of the force field and techniques will require the study of many different systems. We might mention here that the Monte Carlo method has also been used to simulate crystal systems (Hagler & Moult, 1978; Hagler et al., 1980; Mezei et al., 1983); however, in this method the peptide molecules have been held in fixed conformations, and so no information can be gained on their conformational behavior.

Experimental Procedures

Peptide Crystal. *cyclo*-(Ala-Pro-D-Phe)$_2$ crystallizes in the orthorhombic space group $P2_12_12$ with crystallographic twofold axes relating the halves of single peptide molecules and with 2 peptide molecules and 16 water molecules per unit cell (Brown & Teller, 1976). The unit cell parameters are a = 15.908 Å, b = 13.350 Å, c = 9.643 Å, $\alpha = \beta = \gamma = 90°$. The backbone of the peptides is in a double type II β-turn conformation, with L-Pro and D-Phe residues at the corners of the turns (the structure is shown in Figure 4). The alanine residues are in extended conformations (ϕ, ψ = −157°, 172°). There are weak transannular hydrogen bonds (O–N distance = 3.20 Å) between the amide proton of each alanine and the carbonyl oxygen of the opposite alanine. The X-ray study indicated that the water molecules range from fully ordered to fully disordered (Brown & Teller, 1976). The starting system for our studies was constructed by taking the peptide coordinates from the crystal structure and adding waters in random, but sterically reasonable, locations. We chose to place the waters in random locations rather than in the locations observed in the crystal (for the ordered waters) because one of our objectives is to assess the ability of the simulation to reproduce experimental properties. By starting with the waters in random locations, we are not biasing them to the observed positions by the starting configuration and thus provide a far more stringent test of the technique. A Monte Carlo simulation of this system has already been performed (Hagler et al., 1980), and so we shall have an excellent opportunity to compare the results of the two simulation methods. All hydrogen atoms were explicitly included in the system, and a full valence force field (Hagler, 1985) was used to calculate the potential energy and derivatives. The Berendsen SPC water potential (Berendsen et al., 1981) was employed to model the water–water interactions. The nonbonded parameters for the peptide were derived by fitting an extensive set of properties of ≈30 amide and acid crystals including lattice constants, rotation and translation of the asymmetric unit, sublimation energies, energies of dimerization, and dipole moments (Hagler et al., 1974, 1979a,b; Hagler & Lifson, 1974a,b; Lifson et al., 1979; Dauber & Hagler, 1980). The intramolecular parameters used for the peptide–peptide interactions were derived by fitting structures, energies, and vibrational frequencies of model compounds. Peptide–water parameters were taken as the geometric mean of the appropriate water and peptide parameters. A listing of the equation used to calculate the energy of the system and the parameters for this equation is available as supplementary material. The experimental translational symmetry of the system was used to generate the crystal environment through the use of the observed crystal symmetry.

Cutoff Distance. A cutoff distance of 15 Å was applied to nonbond interactions. This is a rather large cutoff when compared to those commonly used in simulations of biological systems, which have typically been in the range 6–8 Å (Karplus & McCammon, 1981; Levitt, 1983; van Gunsteren et al., 1983; Åqvist et al., 1985, 1986; Haneef et al., 1985; Post et al., 1986). The need for a longer cutoff is assessed in Table I, which illustrates the energies and derivatives of interactions between groups of atoms at this distance and compares these with the energies and derivatives of interactions for groups separated by 8 Å. This table shows that the energies are nonnegligible and ≈6 times larger at 8 Å and the derivatives ≈11 times larger than at 15 Å. In order to demonstrate the effect of the cutoff distance on the energy of the peptide system, we have calculated the lattice energy (the intermolecular energy of interaction of a molecule of *cyclo*-(Ala-Pro-D-Phe)$_2$ with all surrounding molecules in its crystal environment) as a function of cutoff distance. The results are shown in Figure 1. This graph shows that, as the cutoff distance increases, the lattice energy is converging at ≈−56 kcal/mol. The energy at a cutoff of 8 Å is −35.2 kcal/mol—only 63% of the value at convergence—whereas with a

Table I: Energies of Nonbond Interactions as a Function of Distance

interacting groups[a]	distance x (Å)	energy[b] (kcal/mol)	derivative[c] (kcal mol^{-1} Å^{-1})
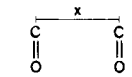	8	+0.1392	−0.0346
	15	+0.0214	−0.0028
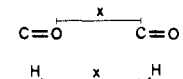	8	−0.1878	+0.0618
	15	−0.0341	+0.0063
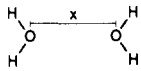	8	+0.2067	−0.0713
	15	+0.0311	−0.0059

[a] Cutoffs are always applied on a group–group basis, where a group is a small set of atoms that have an overall charge of zero. If all atoms in a pair of groups are more than the cutoff distance apart, then the energy of the group–group interaction is ignored. This avoids the problem of sudden appearance or disappearance of unbalanced charges that arises if atom–atom cutoffs are used. [b] This is the energy of the Coulombic interaction. [c] This derivative represents the force acting between the geometric centers of the two groups.

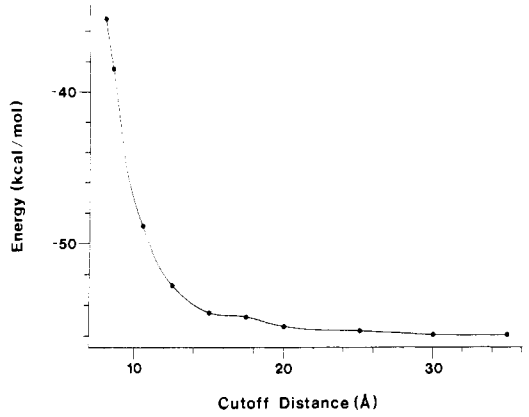

FIGURE 1: Lattice energy of a *cyclo*-(Ala-Pro-D-Phe)$_2$ molecule in its crystal environment varies as a function of the cutoff distance applied to nonbond interactions. The energy is converging at ≈−56 kcal/mol as the cutoff distance increases. With a cutoff of 8 Å the energy is only 63% of this converged value, whereas with a 15-Å cutoff the energy is 97% of the limit.

15-Å cutoff the energy is −54.5 kcal/mol—97% of the converged value. Clearly, then, there is a significant difference between the energies and derivatives of interactions at these different cutoff distances.

The energies and derivatives for the nonbond interactions were switched off over the range 13–15 Å in such a way that they decreased continuously from their full values to zero (Berens et al., 1983).

Minimization and Dynamics Conditions and Convergence Criteria. The energy minimizations were performed by using the conjugate gradient method (Fletcher & Reeves, 1964), and for the molecular dynamics simulations the Verlet algorithm (Verlet, 1967) was used, with a time step of 1 fs. The minimizations and dynamics simulations were run on a Cray X-MP/48 computer system.

The energy of the system was minimized until the average derivative was 0.0005 kcal mol^{-1} Å^{-1}, and the maximum first derivative was 0.0047 kcal mol^{-1} Å^{-1}. The system was then assigned random initial atomic velocities corresponding to a temperature of 298 K, and 100 ps of molecular dynamics were run, during which the average temperature of the system was 307 K. We independently simulated the four asymmetric units of the crystal (i.e., we did not force the system to maintain the crystal symmetry), and thus we can average over these asymmetric units and assess their conformational fluctuations, yielding essentially equivalent information to four separate 100-ps runs (400 ps) on a single asymmetric unit. To investigate whether the dynamics trajectory was exploring only the potential energy well around the minimized crystal conformation or whether it was carrying the system into the region of other minima, minimizations of the energies of the systems reached after 25, 50, 75, and 100 ps were carried out.

Table II: Comparison of Time-Averaged Dynamics Structures of the Four Asymmetric Units of the Crystal of *cyclo*-(Ala-Pro-D-Phe)$_2$ Averaged over Different Time Periods[a]

asymmetric units	time period (ps)				
	0–20	0–40	0–60	0–80	0–100
1, 2	3.377	3.257	3.022	2.615	2.165
1, 3	3.158	3.018	2.959	2.759	2.647
1, 4	2.153	1.956	1.698	1.633	1.722
2, 3	3.965	3.833	3.659	3.594	3.385
2, 4	3.299	3.225	3.139	2.976	2.591
3, 4	2.727	2.838	2.573	2.333	2.246

[a] The numbers given represent the RMS deviation between the torsion angles, in degrees, of the time-averaged structures of the different pairs of asymmetric units of the crystal (asymmetric units 1 and 2 belong to molecule 1, 3 and 4 belong to molecule 2). The waters molecules were not included in the calculations nor were the torsion angles around the C^{α}–C^{β} bond of the alanine residues. The RMS deviations between bond lengths are less than 0.004 Å for all pairs of asymmetric units, and the deviations for the valence angles are all less than 0.5°.

An important consideration in analyzing the dynamics results is whether or not the system has reached equilibrium; that is, has the simulation been run for long enough so that all of the accessible conformational space of the peptides has been visited and all accessible configurational space of the solvent, and has this occurred on the correct time scale. In the case of the crystal simulation, one can take advantage of the symmetry of the system to assess the degree of convergence to an equilibrated state, since, at equilibrium, the time-averaged structure of the four asymmetric units should be the same (Hagler et al., 1980). Table II lists the root mean square (RMS)[1] deviations between corresponding internal coordinates of the peptide molecules for each of the four asymmetric units over different time periods of the simulation. As this table shows, the time-averaged structures of the asymmetric units become more alike as the simulation progresses. For example, the RMS torsion angle difference between asymmetric units 1 and 2 decreases from 3.377° to 3.257° to 3.022° to 2.615° to 2.165° over the first 20, 40, 60, 80, and 100 ps of the simulation. Thus, as we would expect, the system is converging, although the simulation has clearly not been run long enough to reach full convergence. The lack of convergence could be due to two factors: first, that the simulation has not been long enough for the peptides themselves to explore all conformational space available to them or, second, that the positions of the waters have not yet converged on an equilibrium, symmetric (when averaged over a period of time) structure and that this asymmetry of the waters leads to asymmetry of the peptide molecules. The data in Table II and the study of the minimized structures underlying the 25-, 50-, 75-, and 100-ps dynamics structures (see below) show that there is no continuing, systematic movement of the peptides away from their average structure and that they have limited flexibility. Thus, it is reasonable to conclude that in this 100-ps simulation they have had sufficient time to explore the conformational space that is available to them, within the limitations of their own flexibility and of the environment presented by the other peptides and the water structure. As we would expect, the disordered nature of the waters is reflected in their continuous motion during the dynamics. This can be seen from

[1] Abbreviation: RMS, root mean square.

Table III: End-to-End Distances (in Angstroms) Moved by Water Molecules during Different Time Periods of the Molecular Dynamics Simulation of the Crystal of *cyclo*-(Ala-Pro-D-Phe)$_2$

time period (ps)	water no.															
	1	2	3	4	5	6	7	8	9	10	11	12	13	14	15	16
0–25	0.65	2.27	0.92	1.36	1.35	0.34	1.02	1.71	6.11	1.12	2.95	0.28	0.41	0.53	1.82	0.70
25–50	0.61	0.66	1.82	0.70	0.77	3.42	1.66	0.41	0.74	0.71	0.83	0.70	0.40	0.32	0.35	0.86
50–75	0.43	0.25	0.56	0.36	1.36	1.26	1.19	0.87	0.29	1.64	0.28	0.60	0.18	1.19	0.19	0.47
75–100	0.30	0.60	2.71	0.64	0.63	2.20	1.65	0.34	0.46	1.49	0.55	0.53	0.77	2.91	1.16	0.68

Table IV: Ring Torsion Angles for the Experimental Crystal Structure, the 14-ps Instantaneous Structure, and the Time-Averaged Structure from the Isolated Dynamics Simulation of *cyclo*-(Ala-Pro-D-Phe)$_2$, Demonstrating How the Dynamic Fluctuations Bring the Isolated Molecule into a Conformation Close to That Observed in the Crystal

	Ala^1			Pro^2			D-Phe^3			Ala^4			Pro^5			D-Phe^6		
structure	ϕ	ψ	ω	ϕ	ψ	ω	ϕ	ψ	ω	ϕ	ψ	ω	ϕ	ψ	ω	ϕ	ψ	ω
crystal	−157	172	177	−60	122	172	79	9	−169	−157	172	177	−60	122	172	79	9	−169
14-ps dyn[a]	−174	167	160	−48	100	172	100	−66	166	−70	162	−178	−65	110	−161	85	39	−173
time-av dyn	−87	142	−177	−53	109	−164	125	−72	170	−88	151	−180	−62	103	−165	131	−78	172

[a] This is the instantaneous structure visited at the 14-ps time step of the isolated dynamics simulation.

Table III, which shows the distance moved by each water during each 25-ps portion of the dynamics. This table shows that some of the waters, for example, numbers 3 and 14, were still moving considerable distances (2.71 and 2.91 Å, respectively) during the last 25 ps of dynamics, and, in fact, these two water molecules moved further during this 25 ps than during any of the earlier time periods.

Isolated Molecule. In addition to the crystal simulation, we carried out a 100-ps simulation of an isolated molecule of *cyclo*-(Ala-Pro-D-Phe)$_2$ in order to study the conformational fluctuations and dynamics of the isolated molecule and to allow us to determine the effects of packing forces on these properties. A set of coordinates for a single peptide molecule was taken from the experimental crystal structure, and the energy of this isolated molecule was minimized to give the starting coordinates for the simulation. Again, random initial velocities corresponding to a temperature of 298 K were assigned to the atoms. In order to characterize the conformations underlying the dynamics trajectory of the isolated molecule, minimizations were performed on conformations taken at 5-ps intervals throughout the simulation.

Results and Discussion

Behavior of the Isolated Peptide. (a) Visits to Accessible Conformational States during the Dynamics Trajectory. From an inspection of Figure 2, one can see immediately that the peptide favors conformational states in vacuo different from those it favors in the crystal. This figure shows the fluctuations of the ϕ and ψ torsion angles of the two D-phenylalanine residues over the course of the simulation. In the experimentally observed crystal and in the calculated minimum energy crystal that reproduces this feature of the experimental structure, the D-Phe residues occur in the left-handed α-helical (α_L) region of conformational space [ϕ, ψ = 79°, 9° for the experimental structure and 80°, 13° for the minimized structure (molecule 1)]. During the first 3 ps of the simulation of the isolated molecule, these residues undergo a conformational change to the C_7 (equatorial) (ϕ, $\psi \approx 120°, -80°$) region, around which they oscillate for the remaining 97 ps, with the exception of a large fluctuation back to the α-helical state observed in the crystal conformation of the molecule by D-Phe^3 at ≈12 ps and by D-Phe^6 at ≈14 ps. In this conformation at 14 ps the backbone of the peptide has returned close to the experimental structure (with the exception of ψ of D-Phe^3 and ϕ of Ala^4). This is shown in Table IV, which compares the torsion angles of the 14-ps structure with the experimental

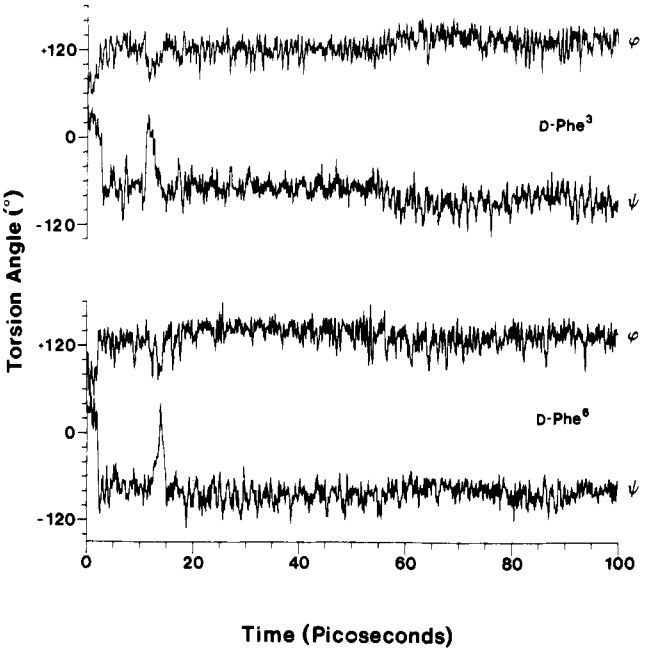

FIGURE 2: Behavior of the two D-phenylalanine residues during the 100-ps in vacuo simulation of *cyclo*-(Ala-Pro-D-Phe)$_2$. The peptide very rapidly changes conformation away from the crystal conformation with which the simulation was started.

values and the time-averaged values for the isolated dynamics simulation. In order to obtain an estimate of the barrier that the molecule has to overcome to reach the structure in which D-Phe^6 is in the left-handed α-helical conformation (the 14-ps structure), the backbone torsion angles from ϕ of Pro^5 to ψ of Ala^1 of the structure obtained by minimizing the energy of the 10-ps dynamics structure were forced to adopt the values of the 14-ps dynamics structure. This was done by performing a minimization in which the energy function was augmented by adding a harmonic term to the energy for the torsion angles to force them to the desired values. By performing a series of minimizations in which the target torsion angles are gradually changed from their values in the starting structure to their values in the final structure, one can obtain an estimate of the maximum barrier to interconversion of the two conformations. This calculation showed that the barrier for interconversion of these two conformations is at most 6.1 kcal/mol. These excursions demonstrate the accessibility of the crystal conformation to the residues in the isolated molecule, even though the crystal conformation is of higher energy.

Table V: Ring Torsion Angles for Minimized Structures of *cyclo*-(Ala-Pro-D-Phe)$_2$ from Trajectory of Isolated Molecule

	Ala^1			Pro^2			D-Phe^3			Ala^4			Pro^5			D-Phe^6		
time (ps)	ϕ	ψ	ω	ϕ	ψ	ω	ϕ	ψ	ω	ϕ	ψ	ω	ϕ	ψ	ω	ϕ	ψ	ω
10	−81	117	−170	−45	113	−160	126	−70	168	−86	168	171	−64	98	−175	126	−76	173
15	−86	168	171	−64	98	−175	126	−76	173	−81	117	−170	−45	113	−160	126	−70	168

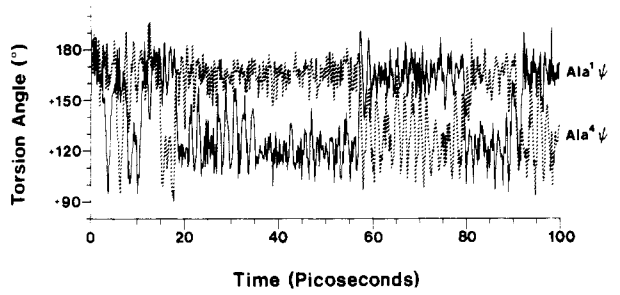

FIGURE 3: Behavior of the ψ torsion angles of Ala^1 (solid line) and Ala^4 (broken line) during the 100-ps in vacuo molecular dynamics simulation of *cyclo*-(Ala-Pro-D-Phe)$_2$. The correlation in the conformational behavior of the two halves of the molecule is illustrated, and it is shown how dynamic transitions in an asymmetric structure can result in a C_2 symmetric structure observed by NMR (see below).

The crystal conformation is visited through dynamic fluctuations, again demonstrating the ability of dynamics to take molecules into higher energy conformations, which may be stabilized by external forces and observed in other systems, such as in the crystal or bound to a receptor.

(*b*) *A Concerted Transition: Differences between Molecular and Spectroscopic Conformations.* At approximately 10 ps into the in vacuo simulation, a concerted conformational change involving the whole molecule takes place. The conformation of residues 4, 5 and 6 flipped to the conformation of residues 1, 2, and 3 prior to the transition, while residues 1, 2, and 3 adopted the conformation of residues 4, 5, and 6. Table V lists the torsion angles for the minimum energy structures underlying the 10- and 15-ps dynamics conformations. The torsion angles for the minimized 10-ps structure correspond to a conformation in which there is a hydrogen-bonded β turn around Pro^2–D-Phe^3, while after the flip, at 15 ps, the β turn is at residues Pro^5–D-Phe^6.

This correlation between the conformation of the two halves of the molecule can be clearly seen in the dynamics (Figure 3). This figure shows the correlation between the ψ torsion angles of Ala^1 and Ala^4. At 10 ps Ala^1 ψ is at $\approx$+120°, while Ala^4 ψ is at $\approx$+170°. Ala^1 ψ then moves to $\approx$+170°, and for a few picoseconds both torsion angles are at approximately this value. At 15 ps Ala^4 ψ moves to the +120° region, completing the flip. After 15 ps, as this figure shows, the molecule settles down to a pattern of oscillation around one pair of values, followed by a rapid flipping of the conformation. This can be seen to take place at $\approx$18, 57, 78, and 91 ps. Although we have only illustrated this for one pair of torsion angles, the same type of behavior can be seen for other pairs. It is interesting to note that if this phenomenon occurred in solution, on the NMR time scale one would observe a 2-fold symmetric structure rather than the instantaneous asymmetric structure. Thus, here we see an example at the molecular level of a conformational averaging process for an asymmetric molecule that would give rise to an average, symmetric spectroscopic structure.

Results of Crystal Minimization and Dynamics. Here we examine several aspects of energy minimization and dynamics simulations of crystal systems, both with respect to the system treated here and in consideration of general features of such simulations: how does the minimized system compare with

Table VI: Comparison of Time-Averaged Dynamics with Minimized Crystal Structures of *cyclo*-(Ala-Pro-D-Phe)$_2$

system	molecule	intramol energy (kcal/mol)	intermol energy[a] (kcal/mol)	RMS torsion angle deviation[b] (deg)
minimized crystal	1	228.7	−87.1	2.162
	2	228.6	−97.9	3.031
minimized from 25-ps dyn	1	228.4	−95.5	2.753
	2	229.0	−95.4	2.022
minimized from 50-ps dyn	1	228.4	−92.1	2.738
	2	228.7	−99.2	2.325
minimized from 75-ps dyn	1	228.4	−92.5	2.723
	2	228.8	−99.1	2.789
minimized from 100-ps dyn	1	228.2	−97.1	2.623
	2	228.8	−97.2	2.051

[a] The energy includes the energy of interaction of the peptide both with other molecules in the basic unit cell and with molecules in translationally related copies of the unit cell up to the cutoff limit. [b] This is the RMS deviation between the torsion angles of the two peptide molecules in the time-averaged dynamics system and the corresponding torsion angles of the peptides in the minimized systems. Torsion angles around the C$^\alpha$–C$^\beta$ bond of the alanine residues were omitted from this calculation. The RMS deviations of bond lengths and valence angles are all less than 0.005 Å and 0.5°, respectively.

that obtained by averaging over each time step of the dynamics (the time-averaged structure) and, most importantly, how do the calculated structures compare with the experimental structure?

(*a*) *Minimized versus Dynamics Crystal Systems.* Table VI compares the time-averaged dynamics crystal system with the minimized crystal system and the systems obtained by minimizing (in the crystal lattice) the energy of the configurations reached at 25, 50, 75, and 100 ps along the dynamics trajectory. Through this type of "quenching" experiment (Stillinger & Weber, 1982, 1983, 1984; Stillinger, 1984; Weber & Stillinger, 1984; Hagler et al., 1985; Struthers et al., 1985) one can examine the stable, minimum energy configurations of the system that underlie the thermally excited, dynamically fluctuating system. These results show that there are distinct minimum energy conformations in which the system can exist, although they are extremely similar to one another and to the time-averaged dynamics structure. They differ from one another mainly in the configurations of the waters of hydration. This suggests that the crystal structure of peptides such as this observed in a diffraction experiment may not represent simply a system fluctuating around a single potential energy minimum but rather an average of a system fluctuating between several similar, yet distinct, minimum energy structures. The similarity between the peptide conformations is shown in Table VI, the intramolecular energies all falling within a 0.8 kcal/mol range and the largest RMS torsion angle deviation from the time-averaged structure being 3.0°. There are, however, large differences in the energy of intermolecular interactions for the peptide molecules. This is indicative of the fact that these small peptides are relatively rigid molecules, especially when constrained by a crystal lattice (as discussed above, greater

Table VII: Torsion Angles of Experimental, Minimized, and Time-Averaged Dynamics Structures of the Crystal of *cyclo*-(Ala-Pro-D-Phe)$_2$

			minimized		time-av dyn	
residue	torsion angle	exptl[a]	molecule 1	molecule 2	molecule 1	molecule 2
Ala[1]	ϕ	−156.6	−148.4	−151.0	−147.8	−146.5
	ψ	171.7	169.9	171.5	170.8	168.9
	ω	177.4	172.7	175.3	173.4	175.2
	χ_1	61.2[b]	53.2	59.3	43.2	55.6
Pro[2]	ϕ	−60.4	−60.4	−59.6	−59.7	−58.5
	ψ	122.5	106.2	106.7	104.6	106.8
	ω	171.6	−171.0	−170.9	−172.6	−171.3
	χ_1	−28.1	−24.8	−27.4	−25.6	−26.3
	χ_2	37.8	35.4	37.0	35.5	35.6
	χ_3	−30.3	−31.7	−31.5	−31.0	−30.5
	χ_4	14.4	16.6	14.8	15.5	14.5
Phe[3]	ϕ	78.7	80.8	80.2	84.6	82.4
	ψ	9.0	12.7	12.7	5.4	5.9
	ω	−169.2	−176.1	−175.1	−175.9	−175.5
	χ_1	63.7	66.8	70.8	68.7	74.6
	χ_2	88.1	83.5	87.2	83.7	90.9
Ala[4]	ϕ	−156.6	−152.4	−151.1	−145.4	−145.2
	ψ	171.7	166.0	167.1	166.9	167.8
	ω	177.4	175.0	171.7	173.3	174.2
	χ_1	61.2[b]	54.7	58.8	132.6	−59.0
Pro[5]	ϕ	−60.4	−57.4	−58.5	−56.1	−59.3
	ψ	122.5	100.4	107.4	101.9	104.1
	ω	171.6	−171.6	−172.4	−172.8	−172.6
	χ_1	−28.1	−27.2	−24.9	−27.4	−25.0
	χ_2	37.8	36.2	35.5	35.8	35.0
	χ_3	−30.3	−30.5	−31.8	−29.6	−30.9
	χ_4	14.4	13.9	16.8	12.8	15.8
Phe[6]	ϕ	78.7	88.1	81.8	86.2	87.1
	ψ	9.0	8.5	8.0	8.5	3.8
	ω	−169.2	−175.4	−176.6	−176.5	−175.7
	χ_1	63.7	68.0	68.4	69.4	69.3
	χ_2	88.1	83.6	81.8	82.5	87.4

[a] The conformations of the two molecules in the experimental crystal structure are identical. [b] The alanine side-chain hydrogens were not located in the crystal structure and so were built on, in a staggered conformation.

conformational freedom was seen for the isolated molecule), but that the solvent environment within the crystal is mobile and changes considerably during the dynamics simulation, resulting in the significant intermolecular energy differences.

(*b*) *Comparison of Calculated with Experimental Crystal Systems.* As we stated above, one of the main objectives in carrying out this type of study is as a test of the force field and the method employed. In Table VII we compare the minimized crystal system and the time-averaged crystal structure obtained from dynamics with the conformation of the peptide in the experimental system. Experimentally, the two peptide molecules in the unit cell of the crystal system are identified with one another. After minimization, however, they are nonidentical. This is because the initial positions of the waters were purposely chosen in a random, asymmetric arrangement in order to provide a more stringent test of the ability of the simulation to reproduce the experimental positions and motions. The asymmetrical arrangement gives rise to asymmetric forces on the peptides during the minimization and therefore to different conformations. It is reassuring to see that the minimized and time-averaged dynamics conformations are close to those of the experimental structure, the RMS differences between the observed crystal and minimized peptide coordinates being 0.29 Å for molecule 1 and 0.32 Å for molecule 2 when all atoms are taken into account and 0.27 and 0.28 Å, respectively, when only non-hydrogen atoms are considered. For comparison, in a recent paper (Hall & Pavitt, 1984) in which the ability of various force fields to reproduce, through energy minimization, the observed crystal structures of three cyclic hexapeptides was evaluated, the RMS differences in non-hydrogen-atom positions ranged from 0.09 to 0.30 Å. In this evaluation, however, the convergence criterion for the energy minimizations was that the energy change over the last 20 cycles of minimization was less than 0.3 kcal/mol, whereas in the present study a much more rigorous criterion was used—all first derivatives were less than 0.005 kcal mol^{-1} Å^{-1} and the energy change over the last 20 cycles was less than 0.5×10^{-5} kcal/mol.

The major differences in torsion angles between the experimental and the calculated (minimized and time-averaged dynamics) crystal structures are in the ψ and ω torsion angles of the proline residues, where the average calculated values are $\langle\psi\rangle = 105°$ and $\langle\omega\rangle = -172°$ compared to observed values of 122° and 172°, respectively. These changes correspond to a slight twisting of the amide group between the Pro and Phe into the plane of the ring (see Figure 4). Other than these, there were no changes in torsion angles of more than about 10°, and the overall shape, including the type II β turns, has been maintained. Thus, the peptide conformation is reproduced extremely well in its crystal environment. More significantly, perhaps, the peptide does not exhibit the large conformational transitions observed in the isolated molecule, indicating the importance of taking into account the appropriate molecular environment.

The peptide molecules started out in their observed conformations. The water molecules, on the other hand, were placed initially in random positions, and several of them moved a considerable distance during the minimization. For the locations in the crystal where waters were accurately located, the fit generally got better. During the dynamics, the waters moved over considerably larger distances than during the minimization (see Table III) but, again, the time-averaged locations of the waters were closer to the experimental locations than were the starting locations. A detailed analysis of water behavior in this crystal will be presented elsewhere.

Effects of the Crystal Environment. In addition to being

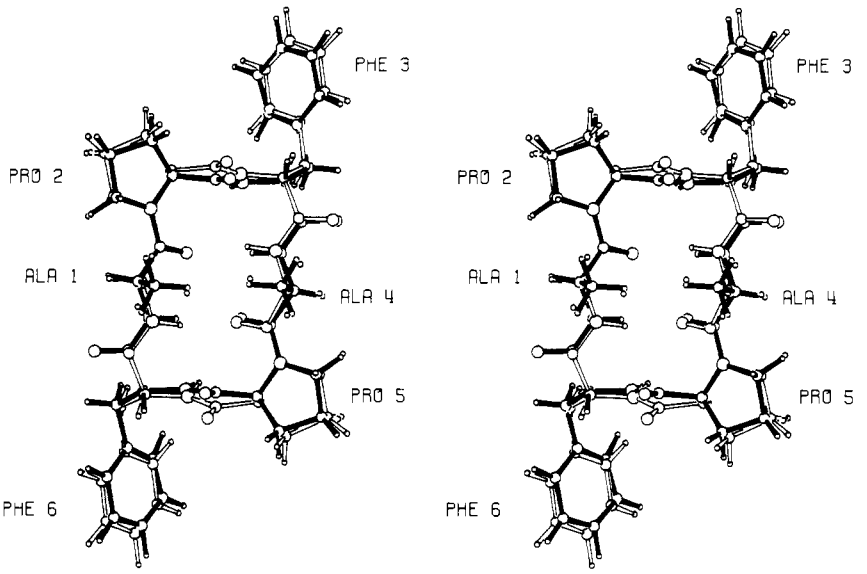

FIGURE 4: Stereoscopic ORTEP (Johnson, 1965) drawing showing the minimized structure (open bonds) of *cyclo*-(Ala-Pro-D-Phe)$_2$ superimposed on the experimental crystal structure (solid bonds).

valuable as tests of the force field, these studies allow us to investigate interesting questions related to the crystal structure itself, for example: Is the peptide in the crystal constrained to a conformation that would be unfavorable in vacuo, and, if so, what intermolecular interactions stabilize it in this conformation? We can attempt to answer this question by comparing the conformations reached during the dynamics simulation of the isolated peptide with the conformation in the crystal system.

(*a*) *Effect of Crystal Forces on the Conformation of the Peptide.* If we compare the minimum energy conformation of the isolated molecule (which was obtained by minimizing the energy of the conformation reached after 60 ps of dynamics in vacuo) with the conformations resulting from minimizing the crystal system, we can see that the crystal forces considerably affect the molecular conformation (see Table VIII). For example, Ala^4 exists in an extended conformation (ϕ, ψ = −152°, 166°) in the crystal (minimized, molecule 1), while in the isolated state it undergoes a transition to the C_7 (equatorial) region (ϕ, ψ = −80°, 117°). Ala^1 goes from ϕ, ψ = −148°, 170° to −86, 167°, and the D-Phe residues have changed from α_L to C_7 as discussed above and seen in Figure 5, which shows the crystal and isolated conformations superimposed on one another. There is still a β turn around Pro^5–D-Phe^6 with a hydrogen bond between the amide hydrogen of Ala^1 and the carbonyl oxygen of Ala^4, but at the other end of the ring there is now a C_7 (equatorial) turn at Pro^2 with a hydrogen bond between D-Phe^3 and Ala^1 (as well as the C_7 turn around D-Phe^3). These changes have resulted in the hexapeptide ring adopting a less planar conformation than in the crystal (Figure 5b). In addition, large changes in the χ_1 torsion angle of the D-Phe residues have led to a significant movement of the phenyl rings. This is illustrated in Figure 5.

(*b*) *Energy.* As we would expect, given the overall similarity of the conformations of the peptide in the two environments, the total (internal plus nonbonded) intramolecular energies of the two structures do not differ dramatically. The intramolecular energies of the peptides in the crystal conformation (228.7 and 228.6 kcal/mol), however, are higher than that of the isolated molecule (220.1 kcal/mol). Thus, these results indicate that the intermolecular interactions, including an extensive network of hydrogen bonds in which the peptides are linked together by bridging water molecules, stabilize the symmetric crystal structure by at least 8.5 kcal/mol (this number could be larger since there may be other conformations of the isolated molecule, of lower energy, that were not visited during the dynamics simulation). It is important to realize that the crystal provides an environment favoring an energetically strained conformation of the peptide. In the case of a biologically active peptide, the receptor will also present such an environment, although this will, of course, be different from that in the crystal.

Table VIII: Torsion Angles of Minimized Crystal and Isolated Structures of *cyclo*-(Ala-Pro-D-Phe)$_2$

residue	torsion angle	minimized[a] molecule 1	minimized[a] molecule 2	isolated minimized
Ala^1	ϕ	−148.4	−151.0	−86.5
	ψ	169.9	171.5	166.7
	ω	172.7	175.3	172.1
	χ_1	53.2	59.3	62.0
Pro^2	ϕ	−60.4	−59.6	−64.8
	ψ	106.2	106.7	93.9
	ω	−171.0	−170.9	−169.5
	χ_1	−24.8	−27.4	−23.4
	χ_2	35.4	37.0	37.3
	χ_3	−31.7	−31.5	−36.0
	χ_4	16.6	14.8	22.3
Phe^3	ϕ	80.8	80.2	136.3
	ψ	12.7	12.7	−84.9
	ω	−176.1	−175.1	173.1
	χ_1	66.8	70.8	167.6
	χ_2	83.5	87.2	96.9
Ala^4	ϕ	−152.4	−151.1	−80.4
	ψ	166.0	167.1	117.3
	ω	175.0	171.7	−170.3
	χ_1	54.7	58.8	62.2
Pro^5	ϕ	−57.4	−58.5	−45.4
	ψ	100.4	107.4	110.7
	ω	−171.6	−172.4	−155.2
	χ_1	−27.2	−24.9	−35.2
	χ_2	36.2	35.5	38.9
	χ_3	−30.5	−31.8	−26.7
	χ_4	13.9	16.8	4.3
Phe^6	ϕ	88.1	81.8	131.7
	ψ	8.5	8.0	−76.8
	ω	−175.4	−176.6	168.0
	χ_1	68.0	68.4	167.1
	χ_2	83.6	81.8	97.5

[a] The two molecules in the minimized crystal system do not have identical conformations since the water molecules were not related by symmetry in the initial configuration (see text).

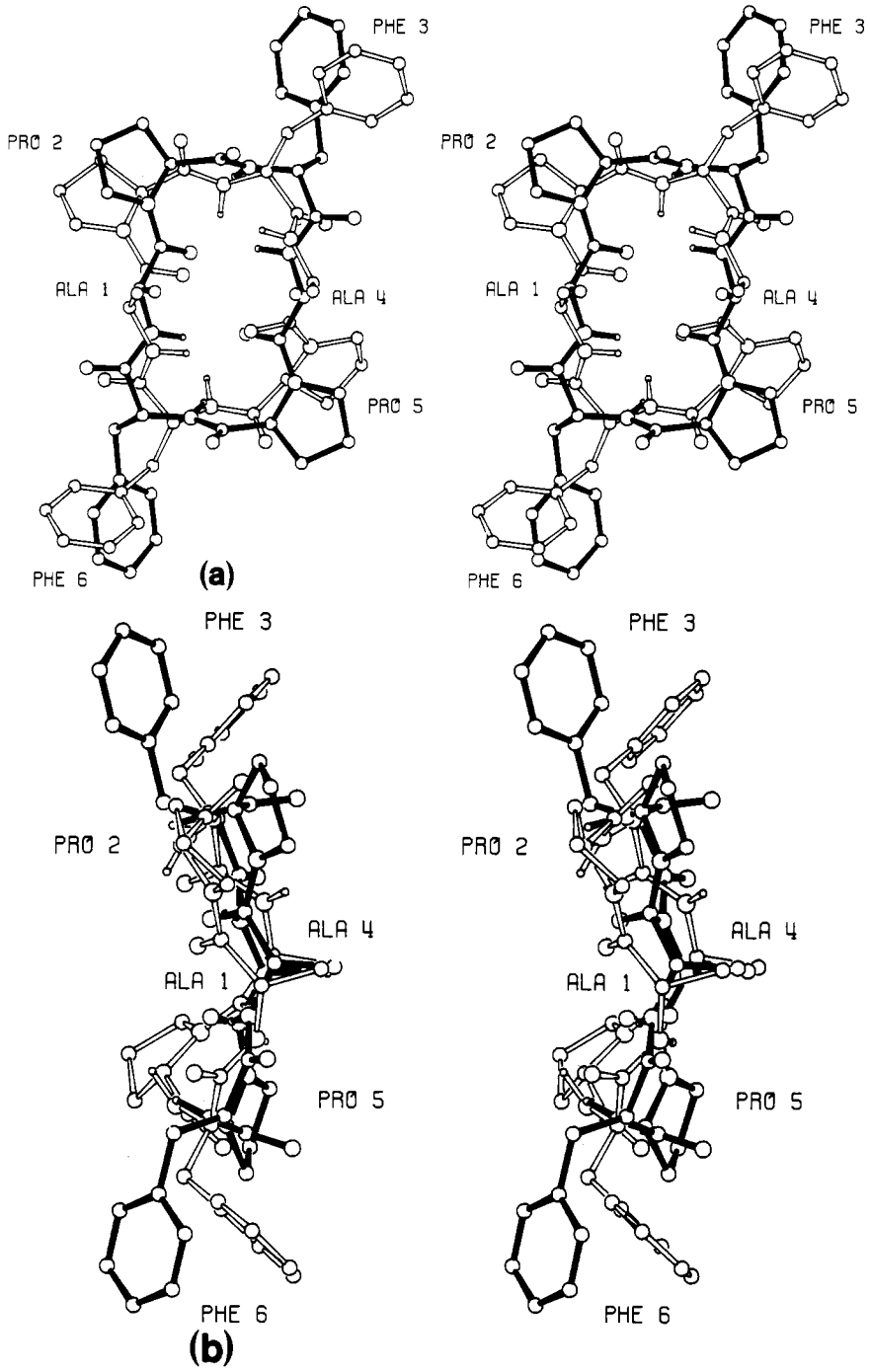

FIGURE 5: Stereoscopic ORTEP (Johnson, 1965) drawings showing the difference between the minimized crystal conformation of *cyclo*-(Ala-Pro-D-Phe)$_2$ (solid bonds) and the lowest energy conformation of the peptide in vacuo (open bonds).

It has been suggested that a C_2 symmetric double β turn conformation of a cyclic hexapeptide requires an unfavorable carbonyl oxygen transannular approach (Madison, 1974; Snyder, 1984). It is interesting to note that the calculated minimum energy conformation of the isolated molecule is not C_2 symmetric. Minimization in vacuo of the (symmetric) peptide from the observed crystal structure leads, of course, to a symmetric conformation (since the minimization algorithm cannot allow a system to lose its symmetry), but this is still 5.4 kcal/mol higher in energy than the minimum energy conformation. In order to calculate the barrier to interconversion of these two conformations, the lowest energy structure was forced to adopt the conformation of the C_2 structure. This was done by performing a minimization of the lowest energy structure in which the energy function was modified by adding the RMS difference in coordinates between this structure and the C_2 structure. By gradually increasing the weighting of the RMS difference so that the structure being minimized is forced to become more and more like the target structure, one can obtain an upper bound to the maximum barrier to interconversion of the two conformations. This experiment indicated that the barrier for going from the lowest energy conformation to the C_2 conformation is about 5 kcal/mol.

(*c*) *Alanine Side Chain Dynamics: Effect of Crystal Forces on Barrier to Rotation.* An example of the information that one can obtain from a dynamics simulation is the nature of dynamic transitions undergone by the molecule. We have already discussed the concerted transition of the molecule as a whole. Here we focus on a localized transition. During the dynamics simulation of the crystal system the alanine residues were seen to undergo rotational transitions reflected by rapid 120° twists around χ (see Figure 6). Rapid spinning of

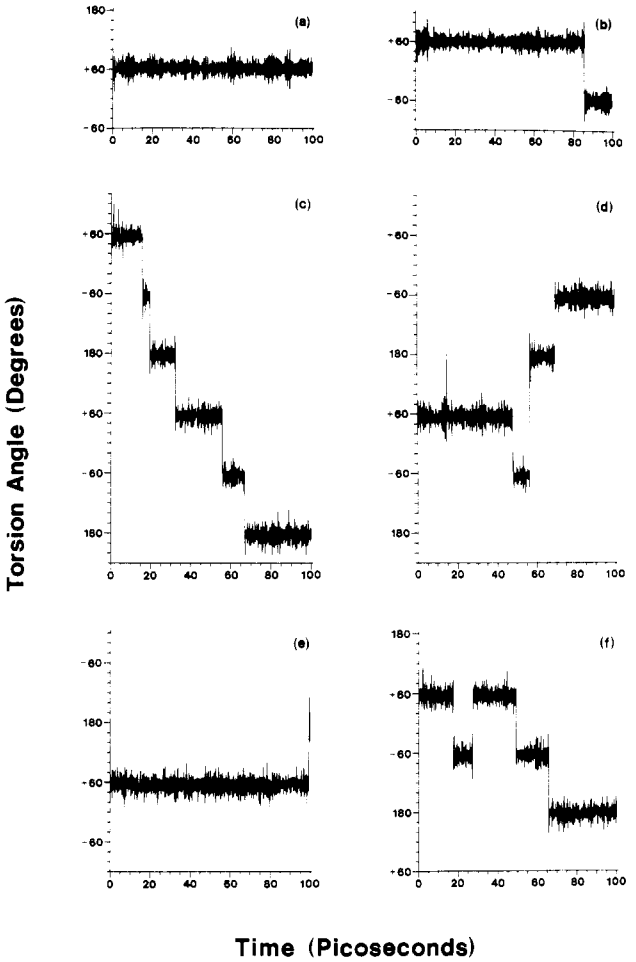

FIGURE 6: Behavior of the alanine side chains during the in vacuo [(a) and (b)] and crystal [(c)–(f)] simulations of *cyclo*-(Ala-Pro-D-Phe)$_2$. The rapid rotations of the methyl group that take place during the dynamics simulations are illustrated. These transitions occur more frequently during the simulation of the peptide in its crystal environment than during the in vacuo simulation, and this is consistent with the lower barrier to rotation calculated for the crystal system (see text).

methyl groups in proteins can be seen experimentally through NMR studies of proteins in solution (Wittebort et al., 1979). In a neutron diffraction study of the protein crambin (Kossiakoff & Shteyn, 1984), the orientations of the methyl groups were studied by sampling the neutron density at 10° intervals around the C_3 rotation axis of each methyl group at the appropriate position for a hydrogen atom. The resulting density profiles indicated that the majority of the methyl groups strongly preferred to adopt a staggered conformation. Thus, the NMR and neutron diffraction data, when considered together, indicate that the methyl groups are undergoing rotations, from one 3-fold energy minimum to the next, with the rotations occurring as very rapid events. This corresponds to the behavior observed in the peptide crystal simulation.

It is interesting to note that only one alanine side-chain rotation of the type described above occurred during the 100-ps simulation of the isolated molecule (see Figure 6), while, on average, there were ≈4 transitions per alanine side chain during the 100-ps crystal simulation (a total of 15 for the 4 asymmetric units simulated independently). That the rotations occur more frequently in the crystal is opposite to what one would intuitively expect and suggests that the main interactions restricting these transitions in this system arise from intramolecular rather than intermolecular contacts and that these interactions must be modulated somehow in the crystal conformation of the peptide (leading to a lower barrier). This was confirmed by calculating the barrier to rotation of the methyl group by the torsion angle forcing method (see above). In the case of the isolated molecule the barrier is ≈4.8 kcal/mol. The contribution from intramolecular interactions to the barrier in the crystal system (where the alanine methyl group on one peptide molecule was forced to rotate) is ≈3.7 kcal/mol, and the contribution from intermolecular interactions of this one molecule with its surroundings is only about 0.1 kcal/mol. Thus, as reflected in the dynamic behavior, the barrier to rotation is lower in the case of the crystal system, and to the extent that the crystal lattice induces the peptide to adopt a conformation which has a lower intramolecular energy barrier, one could say that the crystal is "catalyzing" the rotation of the methyl group. A calculation of the approximate rate of rotation of the methyl groups, at 298 K, which would be expected from the barriers given above, yields 0.19 and 1.02 rotations for the 100-ps trajectory of the isolated and crystal systems, respectively. This is in rough agreement with the 0.5 and 4 rotations per side chain observed in the dynamics. The ratio of the rates calculated from the barriers to rotation, 1:5.4 (isolated:crystal), is also in rough agreement with the ratio seen in the dynamics, 1:7.5, consistent with the dynamics and indicating that the behavior is representative.

Table IX: N–H Stretching Frequencies (in cm^{-1}) of *cyclo*-(Ala-Pro-D-Phe)$_2$ in the Isolated and Crystal States

N–H mode	isolated	crystal
Ala^{1}NH	3440	3426
Phe^{3}NH	3466	3379
Ala^{4}NH	3511	3429
Phe^{6}NH	3503	3484

Table X: Hydrogen Bonds in the Minimized Isolated and Minimized Crystal Structures of *cyclo*-(Ala-Pro-D-Phe)$_2$

donor	acceptor	distance (Å)
isolated		
Ala^1 N–H	Ala^4 C=O	2.1
Phe^3 N–H	Ala^1 C=O	2.3
crystal, intramolecular		
Ala^1 N–H	Ala^4 C=O	2.0
Ala^4 N–H	Ala^1 C=O	2.1
Phe^6 N–H	Ala^4 C=O	2.5
crystal, intermolecular		
Phe^3 N–H	water–16 O	2.0
water–7 H	Pro^5 C=O	1.8
water–9 H	Phe^3 C=O	1.7
water–13 H	Pro^2 C=O	1.8
water–14 H	Pro^5 C=O	1.9

(*d*) *Vibrational Frequencies.* We have calculated the vibrational frequencies of the peptide in both the isolated and crystal states in order to assess the effects of the crystal environment on these frequencies. Table IX compares the N–H stretching frequencies of the isolated peptide and of one of the peptides in the crystal system. One would expect hydrogen bonding to have an effect on the stretching frequencies of bonds involving the hydrogen-bonded atoms. Table X compares the hydrogen-bond interactions in the isolated and crystal systems. One can see from these tables that where an N–H group is involved in a hydrogen bond, there is indeed a lowering of the stretching frequency for that N–H group. For example, Ala^4 N–H is involved in a hydrogen bond (to Ala^1 C=O) in the crystal system but not in the isolated system; the N–H stretching frequency shifts from 3511 cm^{-1} in the isolated molecule to 3429 cm^{-1} in the crystal. The N–H of D-Phe^3 is hydrogen bonded to a water oxygen in the crystal with an H–O distance of 2.0 Å, whereas in the isolated molecule it is involved in a longer hydrogen bond (2.3 Å to the C=O of Ala^1). The

Table XI: Comparison of Experimental Coupling Constants and Torsion Angles (Kopple et al., 1974) with Calculated Values for the Time-Averaged and Minimized Isolated Structures of *cyclo*-(Ala-Pro-D-Phe)$_2$

solvent/calculated system	residue	$J_{\alpha\text{-NH}}$ (Hz)	$\|\theta\|$ (deg)	ϕ (deg)
exptl				
dimethyl sulfoxide	Ala	7.0	145	−155, −85
	D-Phe	7.5	149	89, 151
pyridine	Ala	7.2	146	−154, −86
	D-Phe	8.1	155	95, 145
hexafluoro-2-propanol	Ala	7.4	149	−151, −89
	D-Phe	7.1	146	86, 154
$CDCl_3$	Ala	7.2	146	−154, −86
	D-Phe	8.7	161	101, 139
calcd[a]				
time av[b]	Ala	8.3	166	−87
	D-Phe	6.5	146	128
minimized	Ala	9.0	165	−83
	D-Phe	5.9	136	134

[a] The values given are the average of the two values for the molecule. [b] The value of the coupling constant is the average of the coupling constant calculated at each step of dynamics.

N–H stretching frequency in this case shifts from 3466 cm^{-1} in the isolated state to 3379 cm^{-1} in the crystal. Ala^1 N–H is involved in an intramolecular hydrogen bond in both cases, and there is only a 14-cm^{-1} difference in the frequencies for the two states. Thus, our calculations give rise to the predicted behavior of N–H stretching frequencies in systems involving hydrogen bonds.

NMR Studies: Reinterpretation of Experimental Data in Terms of Conformation. *cyclo*-(Ala-Pro-D-Phe)$_2$ has been studied by NMR in a variety of solvents, including dimethyl sulfoxide, hexafluoro-2-propanol, chloroform, and pyridine (Kopple et al., 1974). The NMR experiment showed that the peptide can exist in two conformations. Both of these forms have C_2 symmetry, the difference lying in the configuration of the Ala–Pro peptide bonds. In the solvents that are poor hydrogen-bond acceptors (chloroform and hexafluoro-2-propanol), only one form, with trans Ala–Pro peptide bonds and good transannular hydrogen bonds, is found. In the other solvents (pyridine and dimethyl sulfoxide), which can form good hydrogen bonds to the peptide protons, signficant amounts of a conformation with cis Ala–Pro peptide bonds were seen (the ratio of trans:cis was 4:1 in pyridine and 1:2 in dimethylsulfoxide).

Using functions that relate the H–N–C$^\alpha$–H coupling constant ($J_{\alpha\text{-NH}}$) to the corresponding torsion angle (θ) (Ramachandran et al., 1971), one can calculate torsion angles from experimental coupling constants or coupling constants for torsion angles in calculated structures. In Table XI the experimentally observed coupling constants, $J_{\alpha\text{-NH}}$ (Kopple et al., 1974), the values of the torsion angles θ derived from these (Ramachandran et al., 1971), and the corresponding values of ϕ calculated on the assumption that $\theta = |\phi - 60|°$ for an L residue and $\theta = |\phi + 60|°$ for a D residue are compared with the values calculated for the time-averaged dynamics and lowest energy minimized structures of the peptide in vacuo. The average of the experimental $J_{\alpha\text{-NH}}$ values is 7.2 Hz for Ala and 7.8 Hz for D-Phe. The corresponding time-averaged values calculated from the dynamics simulation of the isolated molecule are 8.3 and 6.5 Hz. Thus, the calculated values are within ≈1.3 Hz of the observed values. A difference in $J_{\alpha\text{-NH}}$ of 1 Hz, in the region of $J_{\alpha\text{-NH}}$ = 7.4 Hz, corresponds to a difference in θ of only ≈10°, and so we consider the fit of our calculated coupling constants to the experimental values to be reasonable when one takes into account the approximations involved—particularly the lack of solvent in the simulation.

Table XII: Torsion Angles (deg) of NMR, Experimental Crystal, and Time-Averaged and Minimized Isolated Structures of *cyclo*-(Ala-Pro-D-Phe)$_2$

residue	torsion angle	NMR	crystal	time-av isolated dyn[a]	minimized isolated[a]
Ala	ϕ	−150	−157	−87	−83
	ψ	150	172	146	142
Pro	ϕ	−50	−60	−57	−55
	ψ	100	122	106	102
Phe	ϕ	150	79	128	134
	ψ	−40	9	−75	−81

[a] This is the average of the two values for the molecule.

On the basis of the observed coupling constants, conformations were proposed for the peptide with both trans and cis Ala–Pro peptide bonds (Kopple et al., 1974). Table XII compares the torsion angles proposed for the peptide in the trans conformation with the experimental crystal system and the average values of the corresponding torsion angles from the time-averaged dynamics structure and the minimized structure of the peptide in the isolated state. We can see from this table that in some cases (e.g., at Pro) there is good agreement between the NMR, crystal, and calculated isolated conformations. In the case of Phe the isolated molecule is again in the same conformational state as the NMR model, while in the crystal the torsion angles differ considerably. In the case of Ala, however, there is a significant difference in the ϕ torsion angle between the calculated isolated molecule and the NMR structure, while the NMR is in agreement with the crystal conformation. Table XI shows, however, that the observed coupling constant for Ala (≈7.2 Hz) corresponds to two possible ϕ torsion angles (≈−154° and ≈−86°). While the torsion angle chosen for the proposed model (−150°) differs from our simulated structure (−87° for the time-averaged structure), the other possible value (−86°) agrees very well. Thus, our simulated structure can be considered consistent with the experimental data and, in fact, leads to a different interpretation of the experimental results.

Conclusions

As we stated in the introduction, we have several objectives in mind in undertaking this type of study. Our first objective is to test the adequacy and validity of the techniques that we are applying. In this regard, the simulations have shown that, using a combination of molecular dynamics and energy minimization procedures, we can account for the structural properties of a peptide crystal and for the effects of the crystal forces on peptide conformation with a reasonable degree of accuracy. In carrying out the minimizations or molecular dynamics simulations, it is necessary to apply a cutoff to nonbonded interactions. We have investigated the effects of using nonbonded cutoffs of different values and have shown that a value of 15 Å reproduces the true energies and forces significantly more accurately than the more commonly used values of around 8 Å.

Our second objective was to investigate the effects of the crystal environment on the structural, energetic, and dynamic properties of the peptide. The results have shown that the conformation of the peptide is significantly different in the isolated and crystal states, emphasizing that the conformation of a molecule is affected by its environment, so that one must be cautious when attempting to compare results of calculations on isolated systems with experimental crystal structures (Snyder, 1984) or when using crystal structures to rationalize biological activity. The crystal environment has also been shown to have an effect on other features of the system, in-

cluding the rate of rotation of the alanine side chains and the vibrational frequencies of the peptide.

Finally, we have explored our ability to reproduce other types of experimental observables, besides X-ray crystal structures, and have looked at the effect of environment on these observables. The results have shown that the simulations complement experiment and, at least in one case, allowed for the reinterpretation of the spectroscopic data in terms of conformation.

For example, neutron diffraction and NMR studies indicate that alanine side chains within proteins can undergo rapid rotations, and the behavior of the alanine side chains during the dynamics simulations reflects these observations. Similarly, calculations of the effect of the crystal environment on the vibrational frequencies of the peptide reflect the shifts that would be anticipated from experimental studies. We have also calculated NMR coupling constants from the simulation of the isolated molecule and have shown how these calculations could lead to a possible reinterpretation of the experimental data in terms of the conformation of the peptide that was deduced from these data.

Further work remains to be done, including the use of constant pressure dynamics simulations (Andersen, 1980; Nosé & Klein, 1983), tests of our ability to simulate thermal motion by the comparison of calculated with experimental temperature factors, and an extension of this study to a wider range of peptide crystals.

Supplementary Material Available

A listing of the equation used to calculate the energy of the peptide crystal system together with the parameters for this equation (7 pages). Ordering information is given on any current masthead page.

Registry No. *cyclo*-(Ala-Pro-D-Phe)$_2$, 52634-26-1.

References

Andersen, H. C. (1980) *J. Chem. Phys. 72*, 2384–2393.

Åqvist, J., van Gunsteren, W. F., Leijonmarck, M., & Tapia, O. (1985) *J. Mol. Biol. 183*, 461–477.

Åqvist, J., Sandblom, P., Jones, T. A., Newcomer, M. E., van Gunsteren, W. F., & Tapia, O. (1986) *J. Mol. Biol. 192*, 593–604.

Berendsen, H. J. C., Postma, J. P. M., van Gunsteren, W. F., & Hermans, J. (1981) *Jerusalem Symp. Quantum Chem. Biochem. 14*, 331–342.

Berendsen, H. J. C., van Gunsteren, W. F., Zwinderman, H. R. J., & Geurtsen, R. G. (1986) *Ann. N.Y. Acad. Sci. 482*, 269–286.

Berens, P. H., Mackay, D. H. J., White, G. M., & Wilson, K. R. (1983) *J. Chem. Phys. 79*, 2375–2389.

Brown, J. N., & Teller, R. G. (1976) *J. Am. Chem. Soc. 98*, 7565–7569.

Dauber, P., & Hagler, A. T. (1980) *Acc. Chem. Res. 13*, 105–112.

Deslauriers, R., & Smith, I. C. P. (1980) *Biol. Magn. Reson. 2*, 243–344.

Duax, W. L., Hauptman, H., Weeks, C. M., & Norton, D. A. (1972) *Science (Washington, D.C.) 176*, 911–914.

du Vigneaud, V. (1956) *Harvey Lect. 50*, 1.

Fletcher, R., & Reeves, C. M. (1964) *Comput. J. 7*, 149–154.

Hagler, A. T. (1985) in *The Peptides, Analysis, Synthesis, Biology* (Udenfriend, S., & Meienhofer, J., Eds.) Vol. 7, pp 213–299, Academic, Orlando, FL.

Hagler, A. T., & Lifson, S. (1974a) *J. Am. Chem. Soc. 96*, 5327–5335.

Hagler, A. T., & Lifson, S. (1974b) *Acta Crystallogr., Sect. B: Struct. Crystallogr. Cryst. Chem. B30*, 1336–1341.

Hagler, A. T., & Moult, J. (1978) *Nature (London) 272*, 222–226.

Hagler, A. T., Huler, E., & Lifson, S. (1974) *J. Am. Chem. Soc. 96*, 5319–5327.

Hagler, A. T., Dauber, P., & Lifson, S. (1979a) *J. Am. Chem. Soc. 101*, 5131–5141.

Hagler, A. T., Lifson, S., & Dauber, P. (1979b) *J. Am. Chem. Soc. 101*, 5122–5130.

Hagler, A. T., Moult, J., & Osguthorpe, D. J. (1980) *Biopolymers 19*, 395–418.

Hagler, A. T., Osguthorpe, D. J., Dauber-Osguthorpe, P., & Hempel, J. C. (1985) *Science (Washington, D.C.) 227*, 1309–1315.

Hall, D., & Pavitt, N. (1984) *J. Comput. Chem. 5*, 441–450.

Haneef, I., Glover, I. D., Tickle, I. J., Moss, D. S., Pitts, J. E., Wood, S. P., Blundell, T. L., Hermans, J., & van Gunsteren, W. F. (1985) in *Molecular Dynamics and Protein Structure* (Hermans, J., Ed.) pp 85–91, University of North Carolina, Chapel Hill, NC.

Ichiye, T., & Karplus, M. (1983) *Biochemistry 22*, 2884–2893.

Johnson, C. K. (1965) ORNL-3794, Oak Ridge National Laboratory, Oak Ridge, TN.

Karle, I. L. (1981) in *The Peptides, Analysis, Synthesis, Biology* (Gross, E., & Meienhofer, J., Eds.) Vol. 4, pp 1–54, Academic, New York.

Karle, I. L., Karle, J., Wieland, Th., Burgermeister, W., Faulstich, H., & Witkop, B. (1973) *Proc. Natl. Acad. Sci. U.S.A. 70*, 1836–1840.

Karplus, M., & McCammon, J. A. (1981) *CRC Crit. Rev. Biochem. 9*, 293–349.

Kessler, H. (1982) *Angew. Chem., Int. Ed. Engl. 21*, 512–523.

Kopple, K. D., Schamper, T. J., & Go, A. (1974) *J. Am. Chem. Soc. 96*, 2597–2605.

Kossiakoff, A. A., & Shteyn, S. (1984) *Nature (London) 311*, 582–583.

Kuriyan, J., Petsko, G. A., Levy, R. M., & Karplus, M. (1986) *J. Mol. Biol. 190*, 227–254.

Levitt, M. (1983) *J. Mol. Biol. 168*, 595–620.

Lifson, S., Hagler, A. T., & Dauber, P. (1979) *J. Am. Chem. Soc. 101*, 5111–5121.

Liquori, A. M., de Santis, P., Kovacs, A. L., & Mazzarella, L. (1966) *Nature (London) 211*, 1039–1041.

Madison, V. S. (1974) in *Peptides, Polypeptides and Proteins* (Blout, E. R., Bovey, F. A., Goodman, M., & Lotan, N., Eds.) pp 89–98, Wiley, New York.

McCammon, J. A., Gelin, B. R., & Karplus, M. (1977) *Nature (London) 267*, 585–590.

Mezei, M., Beveridge, D. L., Berman, H. M., Goodfellow, J. M., Finney, J. L., & Neidle, S. (1983) *J. Biomol. Struct. Dyn. 1*, 287–297.

Momany, F. A., Corruthers, L. M., McGuire, R. F., & Scheraga, H. A. (1974) *J. Phys. Chem. 78*, 1595–1620.

Northrup, S. H., Pear, M. R., McCammon, J. A., & Karplus, M. (1980) *Nature (London) 286*, 304–305.

Nosé, S., & Klein, M. L. (1983) *Mol. Phys. 50*, 1055–1076.

Post, C. B., Brooks, B. R., Karplus, M., Dobson, C. M., Artymiuk, P. J., Cheetham, J. C., & Phillips, D. C. (1986) *J. Mol. Biol. 190*, 455–479.

Ramachandran, G. N., Chandrasekaran, R., & Kopple, K. D. (1971) *Biopolymers 10*, 2113–2131.

Rose, G. D., Gierasch, L. M., & Smith, J. A. (1985) *Adv. Protein Chem. 37*, 1–109.

Snyder, J. P. (1984) *J. Am. Chem. Soc. 106*, 2393–2400.

Stillinger, F. H. (1984) *J. Phys. Chem. 88*, 6494–6499.
Stillinger, F. H., & Weber, T. A. (1982) *Phys. Rev. A 25*, 978–989.
Stillinger, F. H., & Weber, T. A. (1983) *Phys. Rev. A 28*, 2408–2416.
Stillinger, F. H., & Weber, T. A. (1984) *J. Chem. Phys. 80*, 4434–4437.
Struthers, R. S., Rivier, J., & Hagler, A. T. (1985) *Ann. N.Y. Acad. Sci. 439*, 81–96.
van Gunsteren, W. F., Berendsen, H. J. C., Hermans, J., Hol, W. G. J., & Postma, J. P. M. (1983) *Proc. Natl. Acad. Sci. U.S.A. 80*, 4315–4319.
Verlet, L. (1967) *Phys. Rev. 159*, 98–103.
Weber, T. A., & Stillinger, F. H. (1984) *J. Chem. Phys. 80*, 2742–2746.
Williams, D. E. (1965) *J. Chem. Phys. 43*, 4424–4426.
Wittebort, R. J., Rothgeb, T. M., Szabo, A., & Gurd, F. R. N. (1979) *Proc. Natl. Acad. Sci. U.S.A. 76*, 1059–1063.

Scanning Calorimetric Study of the Thermal Unfolding of Catabolite Activator Protein from *Escherichia coli* in the Absence and Presence of Cyclic Mononucleotides†

Lily R. Ghosaini, Abraham M. Brown, and Julian M. Sturtevant*
Department of Chemistry, Yale University, P.O. Box 6666, New Haven, Connecticut 06511
Received October 27, 1987; Revised Manuscript Received February 24, 1988

ABSTRACT: The thermal unfolding of the catabolite activator protein (CAP) of *Escherichia coli* and the complexes it forms with adenosine cyclic 3′,5′-phosphate (cAMP) and guanosine cyclic 3′,5′-phosphate (cGMP) was studied by high-sensitivity differential scanning calorimetry (DSC). The thermal denaturation of CAP at pH 7.00 gave an irreversible, symmetrical denaturation curve with a single peak. Distinctly different, more complex DSC curves were obtained for the thermal denaturation of the cAMP–protein and cGMP–protein complexes. The DSC data indicate intermolecular cooperation among CAP dimers, with the extent of oligomerization remaining unchanged during unfolding of the protein. The DSC curves for the thermal denaturation of the cAMP–protein complex and cGMP–protein complex have been resolved into three and two components, respectively, according to the model of independent two-state processes. Analysis of the DSC data suggests two and three independent domains for cGMP–protein and cAMP–protein complexes, respectively, with dissociation of mononucleotide occurring in the second component in both cases during protein denaturation. Furthermore, our studies indicate that the presence of either ligand alters the degree of oligomerization of CAP dimers, cAMP having a greater effect than cGMP.

The catabolite activator protein (CAP)[1] or cAMP receptor protein (CRP) of *Escherichia coli* is a well-characterized ligand-induced regulatory protein. The protein complexed with cAMP binds to specific DNA sequences near promoter regions and stimulates transcription (de Crombrugghe et al., 1984).

CAP is a dimeric protein composed of two identical subunits, 22 500 daltons each (Anderson et al., 1971). X-ray crystallographic studies (McKay & Steitz, 1981; McKay et al., 1982) of the cAMP–protein complex to 2.9-Å resolution show that each subunit contains two domains connected by a single covalent stretch of polypeptide: an NH_2-terminal domain that binds cAMP and provides all subunit–subunit contacts and a COOH-terminal domain that binds DNA (Krakow & Pastan, 1972; Eilen et al., 1978). A comprehensive study undertaken by Ebright et al. (1985) involving cAMP, cGMP, and various cAMP analogues reveals changes elicited in the structure of CAP upon nucleotide binding. A greater susceptibility to trypsin cleavage (Krakow & Pastan, 1973) and intersubunit disulfide cross-linking (Eilen & Krakow, 1977) results upon cAMP binding, properties not affected by cGMP. This has been interpreted as indicating that the binding of cAMP to CAP protein elicits a conformational change in the dimer structure while cGMP, which does not stimulate specific DNA binding and transcription, induces no biochemically detected conformational change. The importance of CAP and its complex with cAMP in the transcriptional regulation of some 25 genes in *E. coli* prompted an investigation of the thermodynamics of unfolding of this protein in the absence and presence of either of the ligands, cAMP or cGMP. The isolation and purification of relatively large quantities of CAP protein by a recently developed procedure (Brown, 1987) made possible a study by means of high-sensitivity differential scanning calorimetry. We report here on the thermal unfolding of CAP protein and its complexes with cAMP and cGMP.

Materials and Methods

CAP was isolated from *E. coli* strain HB101 harboring plasmid pHW, a generous gift from Dr. H. M. Wu. The purification and concentration of CAP were carried out on a large scale in a single step by affinity chromatography on cAMP–agarose. Typically, 60 g of cells was suspended in 300 mL of lysis buffer (20 mM sodium phosphate, 20 mM NaCl,

† This research was aided by grants from the National Institutes of Health (GM-04725 to J.M.S. and GM-34205 to D. M. Crothers) and the National Science Foundation (DMB-8421173 to J.M.S.).

[1] Abbreviations: cAMP, adenosine cyclic 3′,5′-phosphate; CAP, catabolite activator protein; CRP, cyclic AMP receptor protein (another term for CAP); DSC, differential scanning calorimetry; DTT, dithiothreitol; EDTA, ethylenediaminetetraacetic acid; cGMP, guanosine cyclic 3′,5′-phosphate.

0006-2960/88/0427-5257$01.50/0